Received: 28 November 2018 | Revised: 28 March 2019 | Accepted: 8 April 2019

DOI: 10.1002/chir.23072

REGULAR ARTICLE

WILEY

Deviations from Beer's law in electronic absorption and circular dichroism: Detection for enantiomeric excess analysis

Qiaozhi Tang[1] | Lu Zhao[1] | Jingqian Xie[3] | Kai Liu[4] | Weiping Liu[1] | Shanshan Zhou[2]

[1]College of Environmental and Resource Sciences, Zhejiang University, Hangzhou, China

[2]College of Environment, Zhejiang University of Technology, Hangzhou, China

[3]College of Marine Ecology and Environment, Shanghai Ocean University, Shanghai, China

[4]Division of Engineering and Applied Science, W. M. Keck Laboratories, California Institute of Technology, Pasadena, California

Correspondence
Weiping Liu, College of Environmental and Resource Sciences, Zhejiang University, 866 Yuhangtang Road, Hangzhou, China.
Email: wliu@zju.edu.cn

Shanshan Zhou, College of Environment, Zhejiang University of Technology, 18 Chaowang Road, Hangzhou 310031, China.
Email: sszhou@zjut.edu.cn

Funding information
National Natural Science Foundation of China, Grant/Award Numbers: 213320102007, 21427815 and 41877494; Natural Science Foundation of Zhejiang Province, Grant/Award Number: LY18B070012

Abstract

The electronic absorption (UV) to circular dichroism (CD) signal ratio can be used for enantiomeric excess (ee) analysis within linear range. However, CD detection often requires a high sample concentration where deviations from Beer's law may occur. Individual enantiomers of four chiral compounds were separated from commercial racemates by semipreparative high-performance liquid chromatography (HPLC) with chiral columns. They were used to trace possible deviations in both UV and CD detection on achiral HPLC with a photodiode array detector and a CD detector. The CD/UV ratios for samples with the same ee value decreased by up to 7.8 to 52% when the injection volume increased, indicating that the linear standard curve of ee versus CD/UV is only valid within a narrow range. To extend the sample amount to a wider range, a data-processing method was developed based on two second-order polynomial functions, which were constructed to fit the relationship between the intensities of the UV and CD signals for two enantiomers. Moreover, a more simplified method based on a third-order polynomial function was established to calculate the ee values. The variations between the predicted and experimental ee values were within ±0.08 for both methods. To our knowledge, this is the first study that the deviations from Beer's law are considered in both UV and CD detection for ee analysis.

KEYWORDS

achiral HPLC, Beer's law, circular dichroism, dual detector, enantiomeric excess

1 | INTRODUCTION

Analysis of chiral composition is crucial in the research areas of pharmaceutical, agrochemical, environmental, life, food, and material sciences.[1-8] Two applicable approaches are commonly used for chiral composition analysis. One is to determine the concentration of each enantiomer after chiral separation.[1-7] The other is to measure the enantiomeric excess (ee) with a circular dichroism (CD) detector.[8-11] The combination of achiral high-performance liquid chromatography (HPLC) separation and CD detection has shown advantages in chiral analysis.[12] For instance, an achiral HPLC-CD system can be used for ee measurements without chiral separation and thus shortens the time required for analysis. Additionally, an HPLC-CD system makes it possible to

simultaneously determine the ee values for many chiral compounds in a complex sample.[13]

In this study, ee is defined as the difference between the enantiomeric fractions (EFs) of two enantiomers:

$$ee = EF_2 - EF_1. \quad (1)$$

In solutions, the EF of each enantiomer is equal to the concentration of one enantiomer divided by the total concentration of the chiral substance. Accordingly, ee can be expressed as

$$ee = (c_2 - c_1)/(c_1 + c_2), \quad (2)$$

where c_1 and c_2 are the concentrations of two enantiomers. For optical detectors, $(c_1 + c_2)$ correlates to the UV absorption signal (*UV*), while the absolute value for $|c_2\text{-}c_1|$ can be seen as the concentration excess of the dominant enantiomer and correlates to the CD signal. Therefore, ee can be measured by UV and CD detection. If Beer's law (the Bouguer-Lambert-Beer Law) is valid and both the UV and CD signals are in linear correlation with the concentration, ee can be determined by

$$ee = k \cdot CD/UV, \quad (3)$$

where *CD* and *UV* refer to the CD and UV signals, and k is a constant.

Beer's law linearly correlates the absorbance to the thickness of the path length and the concentration of the material sample. It has been unquestionably applied to analytical methods related to optical detectors. However, many studies have found that Beer's law only works for analytes with low concentrations and that a nonlinear relationship may exist between the absorbance and the concentration when the analytes are at high-concentration levels.[14,15] These deviations may be ascribed to the occurrence of fluorescence, scattering, physical interactions or chemical equilibrium, the refractive index of the solvent, and many other effects.[14-18] The errors introduced by using Beer's law without correction can easily exceed one order of magnitude, so the limits should be clearly understood before applying Beer's law for any absorbance-related analysis.[19] Because of the low sensitivity of CD detectors for CD detection, a high concentration is often necessary to acquire sufficient CD signals for ee analysis. Therefore, deviations from Beer's law should be carefully monitored and fully considered to determine the ee more accurately.

In this study, the enantiomers of four chiral pesticides, including napropamide (**1**), lactofen (**2**), diclofop-methyl (**3**), and myclobutanil (**4**) were separated from commercial racemates and used to (a) obtain the UV and CD spectra for chiral characterization and wavelength selection for UV and CD detection, (b) trace deviations from Beer's law in their UV and CD signals with increasing compound mass, (c) estimate the influence of these deviations on the determination of ee, (d) establish a nonlinear relationship between the UV and CD signals, and (e) apply the new functions to calculate ee values for samples and evaluate the accuracy. This is the first time that the deviations from Beer's law are observed in both UV and CD detection and considered for CD-related analysis.

2 | MATERIALS AND METHODS

2.1 | Chemicals and materials

Racemic napropamide (**1**), lactofen (**2**), diclofop-methyl (**3**), and myclobutanil (**4**) (all purities >95%) were obtained from Kuaida Agrochemical Co., Ltd. (Jiangsu, China), Nutrichem Co., Ltd. (Zhejiang, China), Yifan Biotechnology Group Co., Ltd. (Zhejiang, China), and Changshu Hengrong Commerce Co., Ltd. (Jiangsu, China), respectively. HPLC-grade solvents, including hexane (Hex), ethanol (EtOH), and isopropanol (IPA), were purchased from Sigma-Aldrich, Shanghai, China. The semipreparative chiral columns (10 × 250 mm, 5 μm), including Chiralcel AD-H, AS-H, OD-H, and OJ-H, were purchased from Daicel Chiral Technologies, China. A normal-phase column packed with bare silica gel (4.6 × 250 mm, 5 μm) was purchased from Welch Materials, Inc. (Shanghai, China).

2.2 | Instruments

Enantiomeric separations of the racemates were run on a Waters semipreparative HPLC system (Milford, MA, USA), including a quaternary gradient module, an autosampler with a 100-μL loop, a column heater, a photodiode array (PDA) detector, and a fraction collector (modules 2535, 2707, 1500, 2998, and WFC III, respectively). The HPLC system was controlled using the Empower software. A Jasco UV-Visible spectrophotometer (V-750) with a 1-cm quartz cuvette was used to record the UV spectra of compounds **1** to **4**. Unitless UV signals (absorbance) were obtained and converted into epsilon (M^{-1} cm^{-1}). A Jasco CD spectrometer (J-1500) with a 1-mm quartz cuvette was used to record the CD spectra of the enantiomers. The CD signals in the unit of millidegrees (mdeg) were obtained and converted into delta-epsilon (M^{-1} cm^{-1}). The analyses of compounds **1** to **4** for ee measurements were performed on a Jasco analytical HPLC system consisting of an autosampler with a 100-μL loop, a quaternary pump, a column oven, a PDA detector, and a CD detector (modules AS-4050, PU-4180, CO-4061, MD-

4010, and CD-4095, respectively). The PDA and CD detectors provided the chromatograms with microvoltage (μV) as the Y-axis units. The ChromNAV control center was used for system control and data acquisition

2.3 | Chromatographic conditions and procedures for chiral separation

The hexane/EtOH and hexane/IPA mixtures were used as mobile phases with flow rate set at 5.0 mL min^{-1} for chiral separation. The specific ratios of the solvent mixtures, the column temperatures, and the chiral columns used for separation for compounds **1** to **4** were listed in Table 1. Racemic chemicals were dissolved into the mobile phases as stock solutions at the concentration of 10 mg mL^{-1}. These solutions were injected at full loop into the semipreparative HPLC. The enantiomeric separations were monitored using the PDA detector with the wavelength range set from 200 to 400 nm (Figure S1). The target peaks of the enantiomers were collected into 250-mL flat-bottomed flasks automatically by setting the acquisition time of the fraction collector. To enhance the enantiomeric purity for each enantiomer, overlapped and tailing portions of the target peaks were not collected. Collected solutions were concentrated by rotary evaporation and then the solvents were further evaporated under a nitrogen flow until a constant weight was reached. The above procedures were carried out repeatedly to obtain sufficient antipodes (>10 mg). Prepared enantiomers were labelled as peak 1 and peak 2 as their elution orders in the chiral separation and were kept in amber bottles and stored at 4°C. The enantiomeric purities of individual antipodes were confirmed under the same chromatographic conditions, with the ee value of each enantiomer >99.9%

2.4 | Measurements for UV and CD spectra

The UV spectra for racemic compounds **1** to **4** and electronic CD spectra for their enantiomers were recorded in hexane solutions. A nitrogen flow with a rate of 20 mL mL^{-1} was introduced into the sample chamber of the CD spectrometer to exclude air and moisture during the measurement. The CD responses of the analytes became overloaded when high-tension voltages of the CD spectrometer were higher than 600 V. To obtain the potentially highest but not overloaded responses, the concentrations of the compounds **1** to **4** were set from 50 to 500 μg mL^{-1} for specific wavelength ranges: For compound **1**, 50 μg mL^{-1} was used within the wavelength range 185 to 260 nm, and 500 μg mL^{-1} was used within 260 to 400 nm; for compound **2**, 250 μg mL^{-1} was used within the wavelength range 185 to 220 nm, and 500 μg mL^{-1} was used within 220 to 450 nm; for compound **3**, 100 μg mL^{-1} was used within 185 to 220 nm, and 500 μg mL^{-1} was used within 220 to 350 nm. For compound **4**, 100 μg mL^{-1} was used within 185 to 210 nm, and 200 μg mL^{-1} within 210 to 250 nm. For shorter wavelength ranges where the CD spectra were noisy, up to 10 cycles of multiple measurements were performed and averaged to smooth the spectra (exemplary graphs shown in Figure S2). The acquired results were calculated, jointed, and finally presented in the unit of delta-epsilon (M^{-1} cm^{-1}).

TABLE 1 Chromatographic conditions for chiral separation of the racemates

Chemicals	Columns	Temp[a] (°C)	Mobile Phases (v/v, %)
Napropamide	OD-H	40	Hex/IPA (85/15)
Lactofen	AD-H	25	Hex/IPA (80/20)
Diclofop-methyl	AS-H	30	Hex/EtOH (98/2)
Myclobutanil	OJ-H	25	Hex/EtOH (90/10)

[a]Temperature set for column heater.

2.5 | Chromatographic conditions and procedures for quantitative analysis

The hexane/EtOH mixture (95:5, v/v) was used as the mobile phase with the flow rate set at 1.0 mL min^{-1} for the quantitative anlysis. The achiral silica gel column was used, and the column oven was set at 25°C. Racemic solutions prepared for compounds **1** to **4** were injected at increasing volumes to test the sample limits. The maximum injected mass of compound **1** to **4** was set to be 0.4, 40, 1.5, and 4 μg, respectively, to avoid obtaining overloaded signals (Figure S3). Enantiopure, racemic, and nonracemic solutions for compounds **1** to **4** were then prepared at the concentrations of 4, 400, 15, and 40 μg mL^{-1}, respectively. The nonracemic solutions were prepared by mixing different ratios and amounts of the enantiopure solutions with the ee values set from −0.8 to +0.8 with an interval of 0.2. The injection volume for the enantiopure, racemic, and nonracemic solutions were set from 1 to 100 μL.

3 | RESULTS AND DISCUSSION

3.1 | Optical characterization and wavelength selection

Wavelength selection is a critical part of method development. The UV and CD spectra were recorded by offline

scanning to find optimal detection wavelengths for further online analysis. As shown in Figure 1, three local maxima are identified in the CD spectrum of compound **1**. The maximum at 230 nm has a higher absolute CD signal (101 deg cm^2 $dmol^{-1}$) compared with the other two at 206 and 242 nm (49.3 and 19.7 deg cm^2 $dmol^{-1}$, respectively). Therefore, 230 nm was selected for CD detection. The UV spectrum of compound **1** exhibits two light absorption maxima at 212 and 290 nm, respectively. In view of the solvent interference for absorbance at lower wavelengths (<220 nm), 290 nm was selected for UV detection. Moreover, 230 nm is also selected in UV detection for compound **1** to make comparison with CD detection. For the *g* (chiral anisotropy factor, calculated by dividing the CD signal by the UV signal at each wavelength) spectrum of compound **1**, the maximum *g* value was located at 246 nm. However, the *g* spectrum near 246 nm was too spiky, and thus, 246 nm is not selected for further discussion. For compound **2**, the CD signal at 230 nm (1.38 deg cm^2 $dmol^{-1}$) is a maximum and approximately double that at 330 nm (0.75 deg cm^2 $dmol^{-1}$). In contrast, the *g* value at 330 nm (37.8) is 7.9 times higher than that at 230 nm (4.81). Thus, we selected 330 nm for further CD detection. For the UV detection of compound **2**, 230 and 280 nm, where light absorption maxima were obtained, as well as 330 nm for CD comparison purposes, are selected. Based on similar selection rules to those of compounds **1** and **2**, the wavelength for CD detection of compound **3** was set to be 280 nm, while for UV, both wavelengths of 230 and 280 nm were selected. In the case of compound **4**, 222 nm was selected for both CD and UV detection. The four chiral compounds that we selected show different wavelengths for CD and UV detection. Moreover, the intensities of the CD and UV signals at those wavelengths are of different magnitude (Table 2). These differences in optical properties can enable one to fully understand the profiles for deviations from Beer's law in

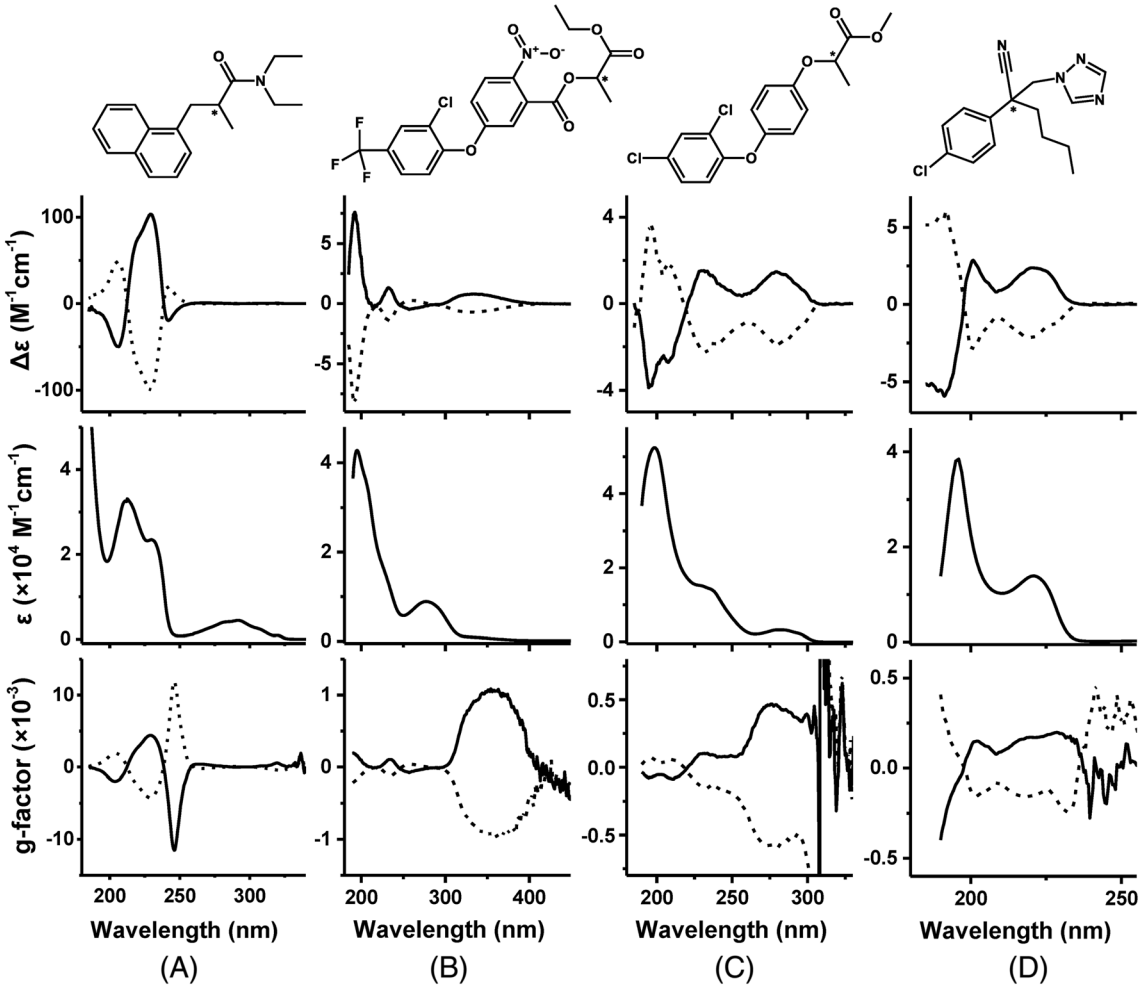

FIGURE 1 Structures and corresponding circular dichroism (CD), electronic absorption (UV), and *g*-factor ($g = CD/UV$) spectra of napropamide (A), lactofen (B), diclofop-methyl (C), and myclobutanil (d). The asterisks in the chemical structures indicate the chiral centers. The CD and *g*-factor spectra for the first eluted peak of two enantiomers are presented as dash lines, and those for the second eluted peak as solid lines

both CD and UV detection with increasing amounts of chiral compounds.

3.2 | Observation of deviations from Beer's law

The UV peak areas for racemic **1** to **4** are plotted against the injected mass in Figure 2. At small sample amounts (injected mass ≤ 0.12, 4, 0.3, and 0.4 μg for compounds **1** to **4**, respectively), the points lie on straight lines that pass through the origin (dot lines in Figure 2). Linear regressions carried out for these points give a value for the square of the correlation coefficients (R^2) > 0.9995, which indicates that the correlations are strictly linear and that Beer's law is obeyed. When the linear regressions are extended to larger sample amounts, the R^2 declines to less than 0.9995, and the deviations are considered to emerge. The maximal deviations are given as percentage values to quantify the decrease in the points from the regression line for the largest sample amount. The UV signals from the CD detector (blue points in Figure 2) show that deviations from Beer's law appear when the injected masses become larger than 0.12, 24, 0.9, and 0.4 μg for compounds **1** to **4**, respectively, which corresponds to approximately 30%, 60%, 60%, and 10% of the largest masses used. In contrast, the UV signals from the PDA detector at the same wavelengths show that deviations appeared when the injected masses were 0.16, 40, 1.5, and 2.4 μg, which corresponds to approximately 80%, 100%, 100%, and 60% of the largest masses used for compounds **1** to **4**, respectively. Moreover, apparent differences were observed between the magnitudes of the deviations for the UV signals measured using the CD detector (blue points in Figure 2) and PDA detector (red points in Figure 2). In detail, the maximal deviations for the UV signals measured using the CD detector were 6.1%, 2.2%, 18%, and 33% for compounds **1** to **4**, respectively, while those for the PDA detector at the same wavelengths were within 2% for compounds **1** to **3**, and 8.9% for compound **4**. These results indicate that in this study, the PDA detector should support wider linear ranges than the CD detector for UV detection when considering reducing the deviations from Beer's law in the UV signals.

It is interesting that the deviations from Beer's law at larger sample amounts can also be found in the CD signals (Figure 3). The maximal deviations for the positive CD signals reached 33.5%, 4.6%, 25.9%, and 66.1% for compounds **1** to **4**, respectively, and those for the negative CD signals were 27.7%, 2%, 16.2%, and 54.8%, respectively. In addition, for the nonracemic solutions prepared in our lab, the deviations from Beer's law exist in both UV and CD detection (Figure S4-7).

3.3 | Influence on ee analysis

Usually, when analysis of ee is performed using an achiral HPLC with a CD detector, a linear standard curve for the CD to UV signal ratio (*CD*/*UV*) versus ee value is determined at a certain concentration.[20] This linear standard curve is valid when the sample amount is within a narrow range where the UV and CD signals are both in linear correlation with the injected mass. In most cases, the deviations from Beer's law for both UV and CD signals were not considered, making it unknown whether this standard curve can be applied to samples at other concentrations. In this study, the *CD*/*UV* ratios (both CD and UV signals were obtained from the CD detector) for various amounts of compounds **1** to **4** were plotted against ee values in Figure 4. At each sample amount, the *CD*/*UV* ratios were linearly correlated with ee values (R^2 > 0.99). However, the regression lines for different sample amounts deviated from each other. As shown in Figure 4, the slopes of the *CD*/*UV* versus ee regression

TABLE 2 Selected wavelengths for CD and UV detection and the optical intensities at corresponding wavelengths

Chemicals	Peak Wavelengths (nm)		ε[b]	Δε[c]	g value[d]
	CD	UV	($M^{-1}cm^{-1}$)	($M^{-1}cm^{-1}$)	
Napropamide	230	230, **290**[a]	2.34×10^4	101	4.32×10^{-3}
Lactofen	330	230, 280, **330**	9.19×10^2	0.754	8.20×10^{-4}
Diclofop-methyl	280	230, **280**	3.20×10^3	1.68	5.25×10^{-4}
Myclobutanil	222	**222**	1.37×10^4	2.17	1.58×10^{-4}

Abbreviations: CD, circular dichroism; UV, electronic absorption.

[a]The bold UV wavelengths were finally selected for ee analysis.

[b]The wavelengths in the CD column on the left were used for the measurement of ε in this table.

[c]Δε is calculated by $\Delta\varepsilon=|\Delta\varepsilon_1-\Delta\varepsilon_2|/2$, where $\Delta\varepsilon_1$ and $\Delta\varepsilon_2$ are the molar circular dichroism for two enantiomers.

[d]g value here is calculated by $g=\Delta\varepsilon/\varepsilon$ for each chiral compound.

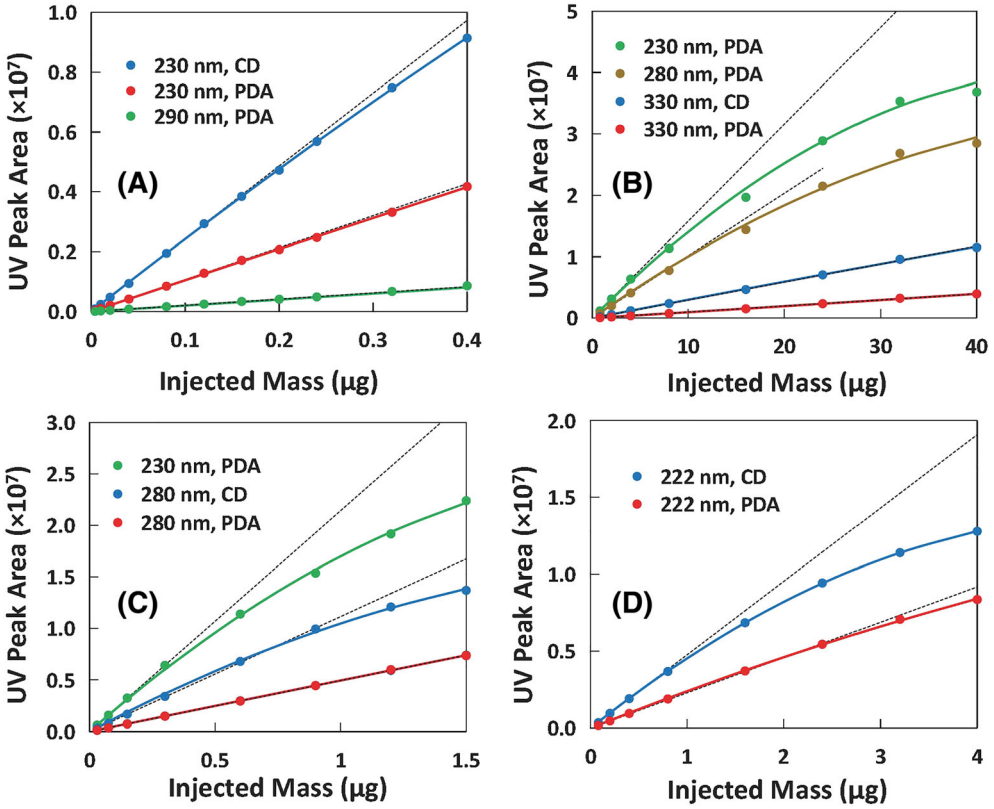

FIGURE 2 The relationship between electronic absorption (UV) peak area and injected mass of racemic napropamide (A), lactofen (B), diclofop-methyl (C), and myclobutanil (D). The measurements were made by the Jasco high-performance liquid chromatography (HPLC) system with circular dichroism (CD) and photodiode array (PDA) dual detectors. The legends show the detection wavelengths and from which detector the data were obtained

lines decreased by up to 28%, 17%, 1.3%, and 41% from the largest slope to the smallest for compounds **1** to **4**, respectively. Meanwhile, the *CD*/*UV* ratios at an ee of 1 decreased from the largest to the smallest by 32%, 12%, 7.8%, and 52% for compounds **1** to **4**, respectively. These results underline the fact that the *CD*/*UV* ratio can vary substantially for varying sample amounts; therefore, using the *CD*/*UV* ratio to measure the ee value is not reliable if the concentrations in samples and standard solutions are different.

The deviation of the *CD*/*UV* ratio is related to the deviations of the CD and UV signals, with the situation possibly very different between compounds. In the case of compound **3**, the maximal deviations for the UV and CD signals were as large as 19% and 25.6% (Figures 2C and 3C), but the *CD*/*UV* versus ee curves at all sample amounts were very close to each other (Figure 4C). The relative standard deviation (RSD) of the slopes was 3.2%, and the standard deviation of the y-intercepts was 0.03. This was because the deviations of the UV and CD signals for compound **3** were both in the decreasing trend (Figures 2C and 3C), leading to smaller deviations of their ratios. In contrast, in the case of compound **2**, the UV and CD signals were well linearly correlated ($R^2 > 0.998$) with the injected mass, but the slope of the curves for *CD*/*UV* versus ee at the largest sample amount increased by 20% compared with that at the smallest sample amount (Figure 4B). It was confusing but also interesting that somehow the CD signals for compound **2** deviated slightly in the increasing trend (Figure 3B) while the UV signals deviated in the decreasing trend (Figure 3B), leading to the considerable deviations of the *CD*/*UV* ratios. Therefore, it is not practical to evaluate or use the linear standard curve for *CD*/*UV* versus ee if the sample and standard solutions are not at the same sample amount.

4 | METHOD MODIFICATIION AND EVALUATION

As described above, the deviations from Beer's law were observed at large sample amounts in both UV and CD detection, and the commonly used standard curve of ee values versus *CD*/*UV* ratios, which was determined at a certain concentration, could not be extrapolated to other concentrations for ee analysis. Therefore, some changes should be made to modify this method. Since the

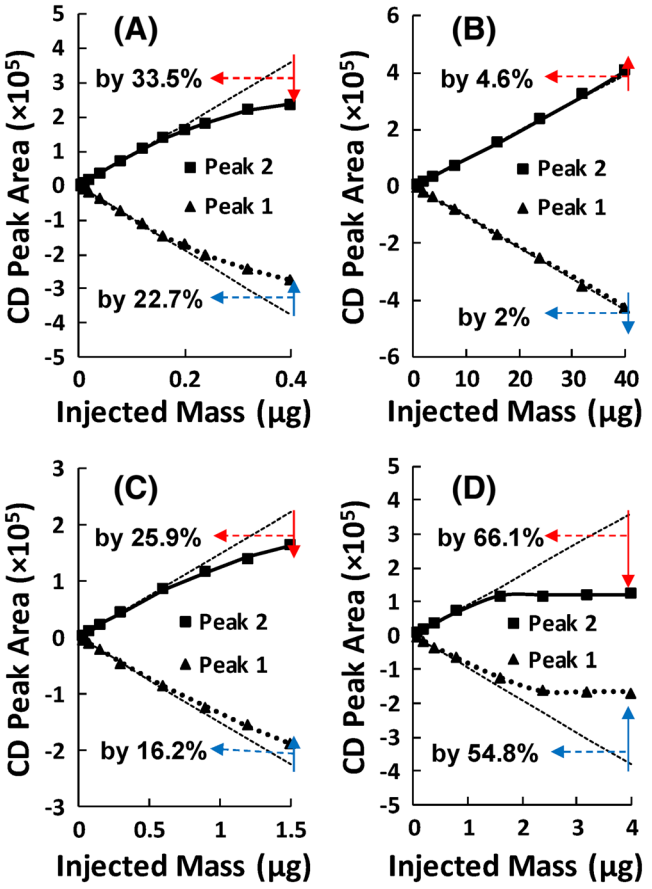

FIGURE 3 The relationship between circular dichroism (CD) peak area and the injected mass of enantiopure napropamide (A), lactofen (B), diclofop-methyl (C), and myclobutanil (D). The wavelengths set for CD detection were 230, 330, 280, and 222 nm for napropamide, lactofen, diclofop-methyl, and myclobutanil, respectively. The dash lines denote linear regression lines generated from small injected masses. The red and blue symbols the percentage numbers denoted that to what percentage the experimental data of CD peak areas deviated from linearily at the largest sample amounts used

deviations of the UV signals with the PDA detector were smaller than those with the CD detector (Figure 2), the UV signals from the PDA detector were used for calculation of the ee. Moreover, in view of the fact that the deviations of the UV signals were smaller at longer wavelengths, the wavelengths for UV detection were selected to be 290, 330, 280, and 222 nm, respectively, for compounds **1** to **4** (Figure 2).

Since the *CD*/*UV* ratios and the ee values were linearly correlated at any certain concentration, as mentioned in the last section, the slope k in Equation 3 can be obtained by UV and CD detection for two pure enantiomers:

$$k = \frac{ee_2 - ee_1}{CD_2/UV_2\text{-}CD_1/UV_1}, \tag{4}$$

or it can be expressed as

$$k = \frac{ee_2 - ee_{\text{sample}}}{CD_2/UV_2\text{-}CD_{\text{sample}}/UV_{\text{sample}}}, \text{ or} \tag{5}$$

$$k = \frac{ee_{\text{sample}} - ee_1}{CD_{\text{sample}}/UV_{\text{sample}}\text{-}CD_1/UV_1}, \tag{6}$$

where ee_{sample}, ee_2, and ee_1 are the ee values of the sample and two pure enantiomers, respectively; CD_{sample}, CD_2, and CD_1 are the CD signals of the sample and two pure enantiomers, respectively; and UV_{sample}, UV_2, and UV_1 are the UV signals of the sample and two pure enantiomers, respectively. Since the total concentrations of the sample and two pure enantiomers are the same, UV_{sample}, UV_2, and UV_1 should all be identical. In addition, because ee_2 and ee_1 are 1 and −1, respectively, the above expressions for the slope k can be combined and expressed as

$$\frac{1 - ee_{\text{sample}}}{CD_2\text{-}CD_{\text{sample}}} = \frac{2}{CD_2 - CD_1}, \text{ or} \tag{7}$$

$$\frac{ee_{\text{sample}} + 1}{CD_{\text{sample}}\text{-}CD_1} = \frac{2}{CD_2 - CD_1}, \tag{8}$$

and thus, the ee value of the sample can be calculated by

$$ee_{\text{sample}} = 1 - \frac{CD_2 - CD_{\text{sample}}}{CD_2 - CD_1} \times 2, \text{ or} \tag{9}$$

$$ee_{\text{sample}} = \frac{CD_{\text{sample}}\text{-}CD_1}{CD_2 - CD_1} \times 2 - 1, \tag{10}$$

where CD_{sample} can be measured directly, and CD_2 and CD_1 are the equivalent CD signals for two pure enantiomers at the same concentration to the sample.

We can obtain CD_2 and CD_1 through three steps: (a) determine the CD and UV signals of two individual enantiomers at various concentrations; (b) associate the CD signals with the corresponding UV signals for two enantiomers by $CD_2 = f_2(UV)$ and $CD_1 = f_1(UV)$, where $f_2(UV)$ and $f_1(UV)$ are two functions of the UV signal; and (c) use the UV signals detected from samples as the arguments of $f_2(UV)$ and $f_1(UV)$ to get CD_2 and CD_1 as the output value, respectively. The expressions of $f_2(UV)$ and $f_1(UV)$ functions were simulated by second-order polynomial curve fittings (Figure 5A) for the four chiral compounds studied, with all values for $R^2 > 0.998$ (Table 3). It should be noted here that the points for compound **4** at the three highest sample amounts were excluded because these points depart from the polynomial fitted curves because of the deformation of their chromatographic CD peaks. Ultimately, we obtained

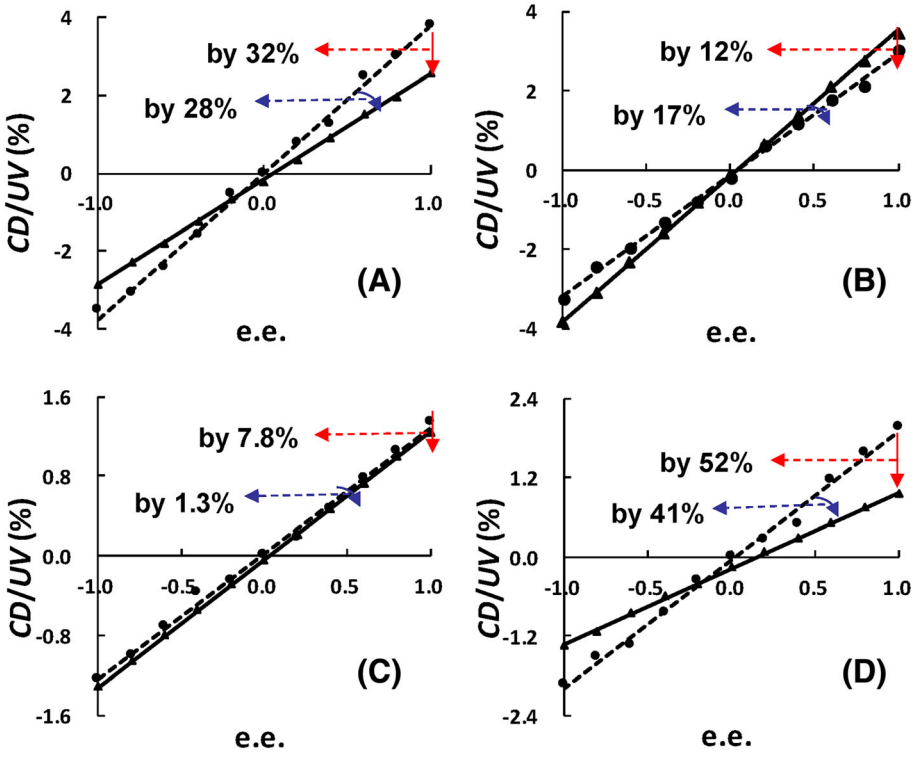

FIGURE 4 Linear standard curves fitted for the data points of the circular dichroism (CD) to electronic absorption (UV) peak area ratios versus the ee values for napropamide (A), lactofen (B), diclofop-methyl (C), and myclobutanil (D). The CD and UV detection wavelengths were 230/290, 330/330, 280/280, and 222/222 nm, for napropamide, lactofen, diclofop-methyl, and myclobutanil, respectively. The data points in circular and triangular are derived from the smallest and largest sample amounts. The red and violet symbols with the percentage numbers denoted that to what percentages the CD to UV peak area ratios and the slopes of the fitted lines decreased when the sample amounts changed with constant ee values of 1

$$ee_{\text{sample}} = 1 - \frac{f_2(UV_{\text{sample}})CD_{\text{sample}}}{f_2(UV_{\text{sample}})\text{-}f_1(UV_{\text{sample}})} \times 2, \text{ or} \quad (11)$$

$$ee_{\text{sample}} = \frac{CD_{\text{sample}}\text{-}f_1(UV_{\text{sample}})}{f_2(UV_{\text{sample}})\text{-}f_1(UV_{\text{sample}})} \times 2 - 1. \quad (12)$$

The ee values for the previously prepared samples (experimental ee) were compared with the ee values calculated by the above equations (predicted ee), with the results shown in Figure S8. The deviations for the predicted ee values were all within ±0.075 compared with the corresponding experimental ee values for compounds **1** to **4**.

Additionally, to simplify the process of analysis, the above method was further modified and another approach developed for ee analysis. For the points with negative CD signals in Figure 5A, a negative sign was introduced for the UV signals by multiplication with the sign function of Sgn (*CD*), which is 1 or −1, depending on whether the sample shows positive or negative CD signals, respectively. The two axes for the UV and CD

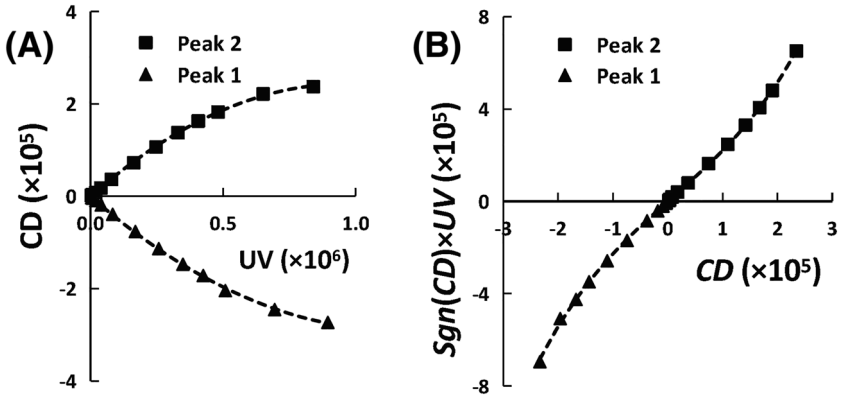

FIGURE 5 The fitted curves with second-order (A) and third-order (B) polynomial fitting curves for enantiopure napropamide. The wavelengths were set at 230 and 290 nm for CD and UV detection, respectively. The CD and UV signals were the peak areas obtained from the analytical high-performance liquid chromatography (HPLC) system

TABLE 3 The second-order polynomial functions fitted to the data points of the CD peak areas ($\times 10^5$) against the UV peak areas ($\times 10^6$) for each enantiomer

Chemicals	Peak	Function	R^2
Napropamide	1	$y=2.1437x^2 - 4.9949x$	0.9994
	2	$y=-2.6007x^2 + 5.046x$	0.9995
Lactofen	1	$y=-0.0025x^2 - 1.1288x$	1.0000
	2	$y=0.0176x^2 + 0.9276x$	0.9999
Diclofop-methyl	1	$y=0.0069x^2 - 0.2927x$	0.9997
	2	$y=-0.0141x^2 + 0.33x$	0.9991
Myclobutanil	1	$y=0.0156x^2 - 0.3953x$	0.9987
	2	$y=-0.0314x^2 + 0.4287x$	0.9988

Abbreviations: CD, circular dichroism; UV, electronic absorption.

signals were exchanged with each other, and the fitted curves of the second-order polynomial function for two enantiomers in Figure 5A connected and merged into one third-order polynomial fitting curve (Figure 5B). These third-order polynomial fitting curves correlate the CD signals of two enantiomer to the signed UV signals. These fittings are shown as

$$\mathrm{Sgn}\,(CD) \times UV = f\,(CD), \tag{13}$$

where $f\,(CD)$ is the output value of the third-order polynomial function of the CD signal (listed in Table 4). Then, a further simplified equation can be obtained as

$$ee = f\,(CD)/UV, \tag{14}$$

which was much easier to be recognized and remembered than the Equation 12.

Equation 14, with the expression of a third-order polynomial function for each chiral compound, was applied to all samples, with a comparison between the predicted and experimental ee values shown in Figure S9. The deviations for the predicted ee values compared with the corresponding experimental ee values were within ±0.08 for compounds **1** to **4**. Therefore, these two modified methods are suitable for accurate ee analysis and can be applied to a wide range of samples under consideration for possible deviations from Beer's law.

TABLE 4 The third-order polynomial functions fitted to the data points of the signed UV peak areas ($\times 10^6$) against the CD peak areas ($\times 10^5$) for each chiral compound

Chemicals	Function	R^2
Napropamide	$y=0.1368x^3 + 0.0475x^2 + 2.1068x$	0.9996
Lactofen	$y=-0.0124x^3 + 0.0451x^2 + 2.9651x$	0.9992
Diclofop-methyl	$y=0.2744x^3 + 0.0649x^2 + 3.4081x$	0.9991
Myclobutanil	$y=0.2744x^3 + 0.0649x^2 + 3.4081x$	0.9994

Abbreviations: CD, circular dichroism; UV, electronic absorption.

5 | CONCLUSION

Deviations from Beer's law were observed in both CD and UV detection for racemates, enantiomers, and nonracemic mixtures of four chiral compounds tested at high concentrations. These deviations hindered extrapolation of the routine method, which is developed at one fixed concentration for ee analysis, to other concentrations. The method was modified depending on second-order fittings of the UV and CD signals obtained for each enantiomer. Another simplified method was developed for the case when deviations from Beer's law in UV detection can be neglected. Comparison of the predicted ee values with the experimental ee values demonstrated that both methods were suitable for accurate ee analysis. These two methods can be used to extrapolate the determination of ee to a wider sample range.

ACKNOWLEDGMENTS

This work was supported by the National Natural Science Foundation of China (21427815, 41877494, and 213320102007) and the Natural Science Foundation of Zhejiang Province (No. LY18B070012).

ORCID

Qiaozhi Tang https://orcid.org/0000-0003-1350-848X
Kai Liu https://orcid.org/0000-0002-2109-8196
Weiping Liu https://orcid.org/0000-0002-1173-892X
Shanshan Zhou https://orcid.org/0000-0002-0050-7739

REFERENCES

1. Zuo ZW, Cong H, Li W, Choi J, Fu GC, MacMillan DWC. Enantioselective decarboxylative arylation of α-amino acids via the merger of photoredox and nickel catalysis. *J Am Chem Soc*. 2016;138(6):1832-1835.
2. Zhang W, Wang F, McCann SD, et al. Enantioselective cyanation of benzylic C-H bonds via copper-catalyzed radical relay. *Science*. 2016;353(6303):1014-1018.
3. Buerge IJ, Müller MD, Poiger T. The chiral herbicide beflubutamid (II): enantioselective degradation and enantiomerization in soil, and formation/degradation of chiral metabolites. *Environ Sci Technol*. 2013;47(13):6812-6818.
4. Andrés-Costa MJ, Proctor K, Sabatini MT, et al. Enantioselective transformation of fluoxetine in water and its ecotoxicological relevance. *Sci Rep*. 2017;7(1):15777.
5. Zhai GS, Hu DF, Lehmler HJ, Schnoor JL. Enantioselective biotransformation of chiral PCBs in whole poplar plants. *Environ Sci Technol*. 2011;45(6):2308-2316.

6. Tarasevych AV, Sorochinsky AE, Kukhar VP, Guillemin JC. Deracemization of amino acids by partial sublimation and via homochiral self-organization. *Orig Life Evol Biosph*. 2013;43(2):129-135.
7. Matheis K, Granvogl M, Schieberle P. Quantitation and enantiomeric ratios of aroma compounds formed by an ehrlich degradation of $_{L}$-isoleucine in fermented foods. *J Agric Food Chem*. 2016;64(3):646-652.
8. Feng WC, Kim JY, Wang XZ, et al. Assembly of mesoscale helices with near-unity enantiomeric excess and light-matter interactions for chiral semiconductors. *Sci Adv*. 2017;3(3):e1601159.
9. Geng L, McGown LB. Determination of enantiomeric excess by fluorescence-detected circular dichroism. *Anal Chem*. 1994;66(19):3243-3246.
10. Song S, Sun L, Yuan L, et al. Method to determine enantiomeric excess of glucose by nonchiral high-performance liquid chromatography using circular dichroism detection. *J Chromatogr A*. 2008;1179(2):125-130.
11. Joyce LA, Sherer EC, Welch CJ. Imine-based chiroptical sensing for analysis of chiral amines: from method design to synthetic application. *Chem Sci*. 2014;5(7):2855-2861.
12. Bertucci C, Tedsco D. Advantages of electronic circular dichroism detection for the stereochemical analysis and characterization of drugs and natural products by liquid chromatography. *J Chromatogr A*. 2012;1269:69-81.
13. Eto S, Yamaguchi M, Bounoshita M, Mizukoshi T, Miyano H. High-throughput comprehensive analysis of $_{D}$- and $_{L}$-amino acids using ultra-high performance liquid chromatography with a circular dichroism (CD) detector and its application to food samples. *J Chromatogr B*. 2011;879(29):3317-3325.
14. Ungnade HE, Kerr V, Youse E. Deviations from Beer's law in the ultraviolet absorption spectra of some organic compounds. *Science*. 1951;113(2943):601.
15. Davenport JB, Houlihan JE, Farina PEL, Forster WA. A departure from Beer's law affecting the spectrophotometric determination of diphenyl. *Analyst*. 1953;78(930):558.
16. Rose HE. Breakdown of the Lambert-beer law. *Nature*. 1952;169(4294):287-288.
17. Buijs K, Maurice MJ. Some considerations on apparent deviations from lambert-beer's law. *J Anal Chim Acta*. 1969;47(3):469-474.
18. Garcia-Rubio LH. Refractive index effects on the absorption spectra of macromolecules. *Macromolecules*. 1992;25(10):2608-2613.
19. Mayerhöfer TG, Mutschke H, Popp J. Employing theories far beyond their limits-the case of the (Boguer-) beer-Lambert law. *J Chem Phys Chem*. 2016;17(13):1948-1955.
20. Lorin M, Delépée R, Ribet JP, Morin P. Validation of a method using an achiral liquid chromatography sorbent and a circular dichroism detector: Analysis of the efaroxan enantiomers. *J Chromatogr A*. 2007;1141(2):244-250.

SUPPORTING INFORMATION

Additional supporting information may be found online in the Supporting Information section at the end of the article.

How to cite this article: Tang Q, Zhao L, Xie J, Liu K, Liu W, Zhou S. Deviations from Beer's law in electronic absorption and circular dichroism: Detection for enantiomeric excess analysis. *Chirality*. 2019;1–10. https://doi.org/10.1002/chir.23072